Numerical modelling of viscoelastic liquids using a finite-volume method

M.S. Darwish and J.R. Whiteman

BICOM, Institute of Computational Mathematics, Department of Mathematics and Statistics, Brunel University, Uxbridge UB8 3PH, UK

M.J. Bevis

Wolfson Centre for Composites, Department of Materials Technology, Brunel University, Uxbridge (UK)

(Received July 23, 1990; in revised form March 27, 1992)

Abstract

A new staggered-grid, finite-volume method for the numerical simulation of isothermal viscoelastic liquids is presented. The main features of this method are the use of a primitive variable formulation, the location of the velocities, pressures and stresses on different staggered grids and the use of a third-order difference scheme for the discretization of the constitutive equations. The method is applied to a sudden-expansion, viscoelastic-flow problem for a range of Weissenberg numbers. For one case the mesh has been refined to demonstrate that the method is robust and viscoelastic effects are not filtered out as the mesh size decreases. All the computations have been performed on a PC equipped with a floating-point coprocessor. Although the method has been defined for, and applied to, two-dimensional problems, the technique is readily extendable to three dimensions without excessive cost.

Keywords: conservation equations; constitutive equations; finite-volume method; numerical modelling; viscoelastic liquids

Correspondence to: J.R. Whiteman, BICOM, Institute of Computational Mathematics, Brunel University, Uxbridge UB8 3PH, UK.

1. Introduction

This paper is concerned with the numerical modelling of the steady-state flow of viscoelastic liquids which exhibit flow phenomena that cannot be explained on the basis of linear or non-linear purely viscous behaviour [1]. This type of modelling requires a mathematical formulation of the problem which adequately represents the physical phenomena and then the discretization of this formulation to produce a numerical algorithm. In a Navier–Stokes model of a purely viscous liquid, use is made of the simple relationship between stress and velocity gradients to write the governing equations in terms of the velocity and pressure. However, for viscoelastic (non-Newtonian) liquids with memory, the relationship between stress and material deformation rates is much more complicated, and the momentum equations contain additional stress terms. The mathematical model used here involves the conservation equations, the equations of continuity and of momentum, and the constitutive equations, which relate stresses to the liquid velocities.

The momentum equations of viscous flow in the Navier-Stokes form contain both hyperbolic terms (the convection terms) and elliptic terms (the diffusion terms) and, depending on the nature of flow, either of these sets of terms can dominate. If the Reynolds number is large, the convection terms are dominant and the momentum equations behave in a hyperbolic manner. Conversely for small Reynolds numbers the diffusion terms are dominant.

In models of viscoelastic liquid flow the situation is additionally complicated due to the above system being further coupled with the (hyperbolic) system of constitutive equations. In any numerical model of viscoelastic liquid flow the discretized forms of all these equations should reflect the features of the systems, otherwise non-physical results will be obtained, and the numerical algorithm will not converge.

Early numerical simulation of viscoelastic liquids involved finite-element techniques based on the Galerkin models of primitive variable formulations, and finite-difference techniques based on stream function-vorticity formulations. The initial developments are reviewed in the book of Crochet et al. [2]. Since then the finite-element techniques have largely been based on mixed methods in terms of velocities, pressure and stress pioneered by Crochet [3,4], and which satisfy the Babuska-Brezzi condition [3], in conjunction with upwinding techniques (streamline upwinding, SU), see, e.g. Brooks and Hughes [5] and Hughes [6], or with less success the SUPG (Streamline Upwinding Petrov Galerkin), see, e.g. Brooks and Hughes [7]. Simultaneously finite-difference methods have evolved to take account of the hyperbolic/elliptic-type changes using switching algorithms between

upwinding (UD) and central differencing (CD), see Song and Yoo [8]. Very recently Yoo and Na [9] have used primitive variables in the finite-difference context with velocity-staggered grids and have been able to obtain results for a Weissenberg number (We) equal to 0.4375 and a Reynolds number (Re) equal to 0.1.

The method developed here involves the use of finite-volume techniques to obtain difference replacements on staggered grids to all the components of the governing equations written in terms of primitive variables. Furthermore, a decoupled approach, whereby the different sets of equations are solved separately, is employed, and in all cases a third-order upwind interpolation profile is used. The primitive variables are the velocity components respectively in the x and y directions u = u[x, y], v = v[x, y], the pressure P = P[x, y], together with stress tensors $\tau^{xx} = \tau^{xx}[x, y]$, $\tau^{yy} = \tau^{yy}[x, y]$ and $\tau^{xy} = \tau^{xy}[x, y]$.

We first state the equations governing the viscoelastic flow, and then describe both the finite-volume discretization and the method of solution of the resulting non-linear equation system. In order to test the algorithm we give in Section 6 results for a problem involving expanding flow for various Weissenberg numbers. For one of the problems the mesh is refined successively to demonstrate that the viscoelastic effects are not filtered out. The results are discussed later in more detail. All the calculations were performed on a Mackintosh SE/30 personal computer.

2. Governing equations

In formulating the viscoelastic flow in terms of the conservation and constitutive equations, we let the liquid occupy the region $\Omega \subset \mathbb{R}^2$. The continuity, momentum and constitutive equations are then respectively:

(a) Continuity equation (conservation of mass) in $\boldsymbol{\Omega}$

$$\frac{\partial}{\partial x}(\rho u) + \frac{\partial}{\partial y}(\rho v) = 0 \tag{1}$$

(b) Momentum equations (conservation of momentum) in Ω

$$\frac{\partial}{\partial x}(\rho uu) + \frac{\partial}{\partial y}(\rho uv) = -\frac{\partial P}{\partial x} + \frac{\partial \tau^{xx}}{\partial x} + \frac{\partial \tau^{xy}}{\partial y}$$
 (2)

$$\frac{\partial}{\partial y}(\rho vv) + \frac{\partial}{\partial x}(\rho vu) = -\frac{\partial P}{\partial y} + \frac{\partial \tau^{yy}}{\partial y} + \frac{\partial \tau^{xy}}{\partial x}$$
(3)

where ρ is the constant density. An alternative formulation for the momentum equations can be written as:

$$\frac{\partial}{\partial x}(\rho uu) + \frac{\partial}{\partial y}(\rho uv) = -\frac{\partial P}{\partial x} + \left[\frac{\partial}{\partial x}\left(\mu\frac{\partial u}{\partial x}\right) + \frac{\partial}{\partial y}\left(\mu\frac{\partial u}{\partial y}\right)\right] + \frac{\partial \underline{\tau}^{xx}}{\partial x} + \frac{\partial \underline{\tau}^{xy}}{\partial y}$$
(4

$$\frac{\partial}{\partial y}(\rho vv) + \frac{\partial}{\partial x}(\rho vu) = -\frac{\partial P}{\partial y} + \left[\frac{\partial}{\partial x}\left(\mu \frac{\partial v}{\partial x}\right) + \frac{\partial}{\partial y}\left(\mu \frac{\partial v}{\partial y}\right)\right] + \frac{\partial \underline{\tau}^{yy}}{\partial y} + \frac{\partial \underline{\tau}^{xy}}{\partial x}$$
(5)

where $\underline{\tau}$ represents only the elastic components of the extra-stress tensor, μ is a viscosity coefficient, and the bracketed terms are correspondingly the viscous terms of the stress tensor. Hence

$$\underline{\tau}^{xx} = \tau^{xx} - 2\mu \frac{\partial u}{\partial x} \tag{6}$$

$$\underline{\tau}^{yy} = \tau^{yy} - 2\mu \frac{\partial v}{\partial y} \tag{7}$$

$$\underline{\tau}^{xy} = \tau^{xy} - \mu \left(\frac{\partial u}{\partial y} + \frac{\partial v}{\partial x} \right) \tag{8}$$

This transformation of the stresses greatly increases the stability of the subsequent numerical calculations and was first introduced by Perera and Walters [10]. The numerical algorithm will be based on eqns. (1) and (4)–(8). In order to be able to solve for u and v in eqns. (1) and (4)–(8), we need constitutive equations which relate stresses to velocity gradients for the viscoelastic liquid.

(c) Constitutive equations in Ω

Two lines of thought can be pursued in the choice of the constitutive equations for the model. One approach is to select fairly simple constitutive equations which contain a minimum number of material parameters, such as the models of Maxwell and Oldroyd, and to concentrate on simulating the flow in this case for as high values of We as is feasible. Another approach is to select more complex constitutive equations which, of course, provide better approximations to the actual behaviour, but which lead to more complicated algorithms. In the present paper, we shall concentrate on the first approach and use the Upper-Convected Maxwell fluid model in which the constitutive equations, written in conservation form, are

$$\frac{\partial(\lambda u \tau^{xx})}{\partial x} + \frac{\partial(\lambda v \tau^{xx})}{\partial y} = 2\mu \frac{\partial u}{\partial x} - \left(1 - 2\lambda \frac{\partial u}{\partial x}\right) \tau^{xx} + 2\lambda \frac{\partial u}{\partial y} \tau^{xy} \tag{9}$$

$$\frac{\partial(\lambda u \tau^{yy})}{\partial x} + \frac{\partial(\lambda v \tau^{yy})}{\partial y} = 2\mu \frac{\partial v}{\partial y} - \left(1 - 2\lambda \frac{\partial v}{\partial y}\right) \tau^{yy} + 2\lambda \frac{\partial v}{\partial x} \tau^{xy} \tag{10}$$

$$\frac{\partial(\lambda u \tau^{xy})}{\partial x} + \frac{\partial(\lambda v \tau^{xy})}{\partial y} = \mu \left(\frac{\partial v}{\partial x} + \frac{\partial u}{\partial y} \right) - \tau^{xy} + \lambda \frac{\partial u}{\partial x} \tau^{xx} + \lambda \frac{\partial v}{\partial x} \tau^{yy}$$
(11)

where λ is the relaxation time.

It is worth noting that if transformations (6)–(8) are used, the momentum equations reduce to the Navier–Stokes form when $\lambda = 0$, because the extra-stress tensors $\underline{\tau}^{xx}$, $\underline{\tau}^{yy}$ and $\underline{\tau}^{xy}$ are zero.

3. Discretization

3.1 The staggered grid

In the finite-volume discretization, the finite-difference approximations to the continuity, momentum and constitutive equations will be set up here using control volumes, ΔV , (or finite volumes) surrounding each grid point. The differential equation is then integrated over the control volume of each variable and piecewise profiles expressing the variation of the variable are used in the integrals to replace boundary values by volume-centred values. In this formulation quantities such as mass and momentum are conserved over every control volume and hence over Ω (see, e.g. Ref. 11).

The above discretization approach leads to staggered grids, as the different dependent variable derivatives are approximated at different mesh points. For example, in our staggered grid, the velocity components are calculated for the points that lie on the faces of the pressure control volumes (see Fig. 1). Thus the u locations are staggered only in the x-direction, and the v locations only in the y-direction. Furthermore the

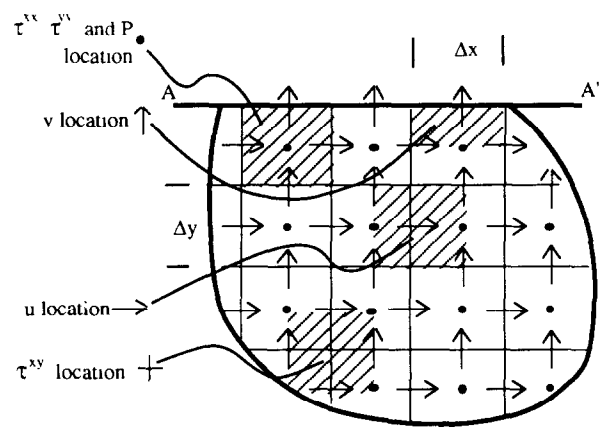


Fig. 1. Control volumes and staggered grid with the dependent variables.

shear stress τ^{xy} locations are staggered as shown, while the pressure and the normal stresses are located on the main grid, which is the square grid surrounding each mesh point, \bullet , of Fig. 1.

The reasons behind this arrangement for the stresses are as follows:

- (a) Since the constitutive equations are complicated and cannot be replaced by a simple function of velocity and viscosity, the stresses need to be included as unknowns together with the primary variables u, v and P; this is done at the main grid for τ^{xx} , τ^{yy} and at the offset grid for τ^{xy} .
- (b) As the use of the stress values is inescapable, they are treated in this way in order to avoid the use of interpolation in the momentum equations. In Fig. 1, AA' is a segment of the boundary of Ω on which the normal velocity is prescribed, whilst the stresses are derived analytically.

3.2 The discretized equations

All of the governing continuity, momentum and constitutive equations (changed into conservative form) can be written in the form of a general equation where the different symbols have different meanings in different contexts. This is

$$\frac{\partial}{\partial x} \left(\rho u \phi - \Gamma \frac{\partial \phi}{\partial x} \right) + \frac{\partial}{\partial y} \left(\rho v \phi - \Gamma \frac{\partial \phi}{\partial y} \right) = S_{\phi}$$
 (12)

with the appropriate terms put into S_{ϕ} .

Equation (12) will be discretized using the control-volume methodology. The discretization takes place at two levels. In level I, the equations are integrated over the control volume so as to get a discretized description of the conservation laws. In level II an interpolation profile is used to relate the terms discretized in level I to the discrete nodes on the solution domain. We consider the x- and y-derivative terms in eqn. (12) separately. (a) Level I discretization

Integrating eqn. (12) over a control volume yields:

$$\int_{b}^{t} \int_{l}^{r} \left[\rho \frac{\partial u \phi}{\partial x} - \frac{\partial}{\partial x} \left(\Gamma \frac{\partial \phi}{\partial x} \right) \right] dx dy + \int_{l}^{r} \int_{b}^{t} \left[\rho \frac{\partial v \phi}{\partial y} - \frac{\partial}{\partial y} \left(\Gamma \frac{\partial \phi}{\partial y} \right) \right] dy dx$$

$$= \int_{\Delta V} S_{\phi} dV \tag{13}$$

Using the divergence theorem, we get for the individual terms of eqn. (13):

I:
$$\int_{b}^{t} \left[\left(\rho u \phi - \Gamma \frac{\partial \phi}{\partial x} \right)_{r} - \left(\rho u \phi - \Gamma \frac{\partial \phi}{\partial x} \right)_{t} \right] dy$$
 (14)

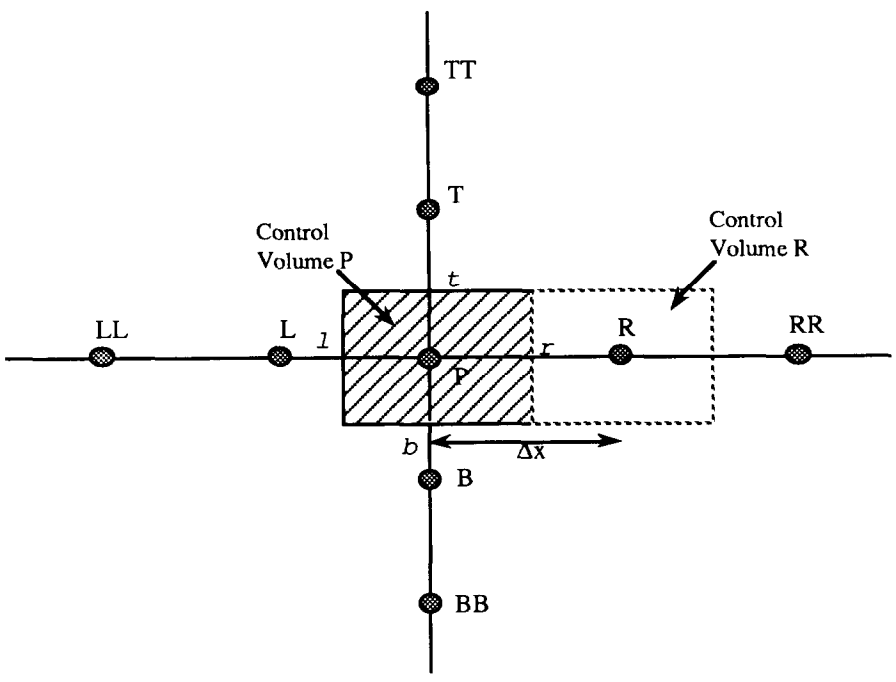


Fig. 2. The discretization molecule with control volume for point P.

II:
$$\int_{l}^{r} \left[\left(\rho v \phi - \Gamma \frac{\partial \phi}{\partial y} \right)_{t} - \left(\rho v \phi - \Gamma \frac{\partial \phi}{\partial y} \right)_{b} \right] dx$$
 (15)

III:
$$\int_{\Delta V} S_{\phi} \, dV \tag{16}$$

where the subscripts l, r, b and t indicate the left, right, bottom and top faces respectively, see Fig. 2. Term I represents the total flux of ϕ leaving the control volume across the r face, and entering the control volume across the l face. Similarly for term II in the y direction. Term III represents different phenomena depending on ϕ .

Each of the integral terms on the left-hand side of eqn. (13) represents a transport by convection and diffusion through the relevant control-volume face. Thus if we denote this quantity for the r face as \tilde{F}_r , then

$$\tilde{F}_r = \int_b^t \left(\rho u \phi - \Gamma \frac{\partial \phi}{\partial x} \right)_r \, \mathrm{d}y \tag{17}$$

Similar expressions can be applied to the other faces of the control volume. The integration indicated by eqn. (17) may be approximated by:

$$F_r = \left(\rho u \phi - \Gamma \frac{\partial \phi}{\partial x}\right)_r \Delta y \tag{18}$$

where the subscript r is interpreted to signify best-estimate values representative of the right face of the control volume for P in Fig. 2. Expressions similar to eqn. (18) may be written for the other faces. Thus after some manipulation, eqn. (13) is approximated by:

$$F_r - F_l + F_t - F_b = \int_{\Delta V} S_\phi \, dV \tag{19}$$

(b) Level II discretization

As can be seen from eqn. (19) the accuracy of the control-volume solution depends on the proper estimation of the face value of ϕ as a function of the neighbouring ϕ node values. Through the use of a profile assumption or interpolation profile, which is an estimate of this variation of ϕ between the nodes, the approximation scheme produces an expression for the face value which is dependent on the nodal ϕ values in the vicinity of the face.

A similar application for an approximation scheme on the other faces of the control volume, and the substitution into eqn. (19) of the expressions obtained, results in an equation relating ϕ_P to its neighbouring nodal values, the control-volume equation of the control volume for P, which may be symbolically represented by:

$$A_{\mathrm{P}}\phi_{\mathrm{P}} = \sum_{\mathrm{nb}} A_{\mathrm{nb}}\phi_{\mathrm{nb}} + B_{\mathrm{P}} \tag{20}$$

For each differential equation, the totality of all equations such as (20) for every control volume in the solution domain constitutes the equation set to be solved for $[\phi_P]$. In eqn. (20) the subscript nb refers to neighbours of P. The term B_P is a source term associated with the control volume P which parallels the source term S_{ϕ} of eqn. (13).

We now describe in detail the profile assumption adopted in this study.

3.3 The interpolation profile

A number of interpolation profiles have been proposed for the approximation of expressions such as (18), see Ref. 12. While all the schemes use central differencing for the approximation of the diffusion term in (18), namely:

$$\left. \frac{\partial \phi}{\partial x} \right|_{r} = \frac{\phi_{R} - \phi_{P}}{\Delta x},\tag{21}$$

it is in the approximation of the convection term that the schemes differ. The simplicity of the convection term is highly deceptive and its approximation remains one of the central issues of computational fluid dynamics [12].

During the 1970s the most widely used scheme was the hybrid differencing scheme [13]. However, its lack of accuracy due to false diffusion [14] led to the development of new approximation schemes such as the skew upwind differencing scheme (SUDS) of Raithby [15] and the quadratic upstream interpolation for convective kinematics scheme (QUICK) of Leonard [16].

The scheme adopted in the present study is a modification of the QUICK scheme and was developed by Gaskell and Lau [17] under the acronym SMART (Sharp and Monotonic Algorithm for Realistic Transport). The QUICK scheme is first presented, then the SMART scheme is described.

The method developed by Leonard is based upon interpolating the value of the dependent variable at each face of the control volume by using a second-degree (quadratic) polynomial biased toward the upstream direction. The interpolated value is used to calculate the convective term in the governing equations for the dependent variable. The calculation of the values of the dependent variable at the right face of the control volume shown in Fig. 2 is given in detail.

In its original form, the QUICK scheme required the use of a general second-degree polynomial for the calculation of the unknown ϕ_r

$$\phi(x, y) = C_0 + C_1 x + C_2 x^2 + C_3 y + C_4 y^2 + C_5 xy$$
(22)

However, it is generally unnecessary to consider interpolation in the transverse direction [18] so that for the calculation of the unknown ϕ we have

$$\phi(x) = K_0 + K_1 x + K_2 x^2 \tag{23}$$

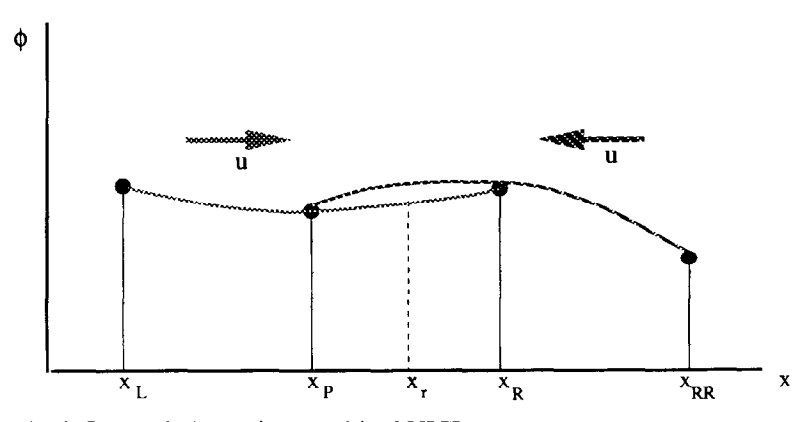


Fig. 3. Interpolation points used in QUICK.

Equation (23) can be rewritten in a more convenient form for a point lying on the right face of control volume P as:

$$\phi_r = C_0 + C_1(x_r - x_p) + C_2(x_r - x_p)(x_r - x_R)$$
(24)

Consider the situation for a positive axial velocity u (see Fig. 3) in which case the values of ϕ at the nodes L, P and R are used to evaluate C_0 , C_1 and C_2 so that

$$\phi_r^+ \equiv \phi_P + \frac{\phi_R - \phi_P}{x_R - x_P} (x_r - x_P) + \left(\frac{\phi_P - \phi_L}{x_P - x_L} - \frac{\phi_R - \phi_P}{x_R - x_P} \right) \frac{(x_r - x_P)(x_r - x_R)}{x_L - x_R}$$
(25)

For the case where the axial velocity is negative, the coefficients C_0 , C_1 and C_2 are calculated using the values of ϕ at grid nodes P, R, RR so that

$$\phi_r^- \equiv \phi_P + \frac{\phi_R - \phi_P}{x_R - x_P} (x_r - x_P) + \left(\frac{\phi_{RR} - \phi_P}{x_{RR} - x_P} - \frac{\phi_{RR} - \phi_P}{x_{RR} - x_P} \right) \frac{(x_r - x_P)(x_r - x_R)}{x_{RR} - x_R}$$
(26)

For the case of a uniform grid, eqns. (25) and (26) take the following form:

$$\phi_r^+ = \frac{1}{2}(\phi_R + \phi_P) - \frac{1}{8}(\phi_R - 2\phi_P + \phi_L)$$
 (27)

$$\phi_r^- = \frac{1}{2}(\phi_P + \phi_R) - \frac{1}{8}(\phi_{RR} - 2\phi_R + \phi_P)$$
 (28)

As the velocity u determines the interpolation points, we define a flow velocity direction switch:

$$d_r^{u+} \equiv \frac{1 + |u_r|/u_r}{2} \text{ and } d_r^{u-} \equiv 1 - d_r^{u+}$$
 (29)

so that the value of ϕ_r at the control-volume face becomes

$$\phi_r = d_r^{u+} \phi_r^+ + d_r^{u-} \phi_r^- \tag{30}$$

The value of ϕ at other faces is calculated analogously.

Difficulties arise in using the QUICK scheme due to its unboundedness; that is there is a tendency for overshoot and undershoot values to be generated under large gradients. The modification introduced by Gaskell and Lau [17] for overcoming this unboundedness amounts to the addition of a variable parameter to the curvature term (e.g. the second term in the

right-hand side of eqns. (27) and (28)) of the QUICK scheme. Thus equations (27) and (28) become:

$$\phi_r^+ = \frac{1}{2}(\phi_R + \phi_P) - (\frac{1}{8} + \alpha_r)(\phi_R - 2\phi_P + \phi_L)$$
(31)

$$\phi_r^- = \frac{1}{2}(\phi_P + \phi_R) - (\frac{1}{8} + \alpha_r)(\phi_{RR} - 2\phi_R + \phi_P)$$
 (32)

where the α_r depend on the normalized values $\tilde{\phi}$ of ϕ [19] which are defined in the Appendix along with their relation to α_r . Similar parameters are used for other faces.

3.4 The coefficients of the general control-volume equation

If we are to calculate $F_r - F_l$ in eqn. (19), we have by definition

$$F_r - F_l = \left(\rho u\phi - \Gamma \frac{\partial \phi}{\partial x}\right)_r \Delta y - \left(\rho u\phi - \Gamma \frac{\partial \phi}{\partial x}\right)_l \Delta y \tag{33}$$

Defining

$$C_r = \rho u_r \, \Delta y \qquad C_l = \rho u_l \, \Delta y$$

$$D_r = \mu_r \frac{\Delta y}{\Delta x} \qquad D_l = \mu_l \frac{\Delta y}{\Delta x} \tag{34}$$

eqn. (33) becomes, after replacing the diffusion term using eqn. (21),

$$F_r - F_l = C_r \phi_r - C_l \phi_l + (D_r + D_l) \phi_P - D_r \phi_R - D_l \phi_L$$
(35)

where

$$C_{r}\phi_{r} - C_{l}\phi_{l} = C_{r}(d_{r}^{u+}\phi_{r}^{+} + d_{r}^{u-}\phi_{r}^{-}) - C_{l}(d_{l}^{u+}\phi_{l}^{+} + d_{r}^{u-}\phi_{l}^{-})$$

$$= C_{r}\left\{d_{r}^{u+}\left[\frac{\phi_{R} + \phi_{P}}{2} + \left(\frac{1}{8} + \alpha_{r}\right)(2\phi_{P} - \phi_{R} - \phi_{L})\right] + d_{r}^{u-}\left[\frac{\phi_{R} + \phi_{P}}{2} + \left(\frac{1}{8} + \alpha_{r}\right)(2\phi_{R} - \phi_{P} - \phi_{RR})\right]\right\}$$

$$- C_{l}\left\{d_{l}^{u+}\left[\frac{\phi_{L} + \phi_{P}}{2} + \left(\frac{1}{8} + \alpha_{l}\right)(2\phi_{L} - \phi_{P} - \phi_{LL})\right] + d_{l}^{u-}\left[\frac{\phi_{L} + \phi_{P}}{2} + \left(\frac{1}{8} + \alpha_{l}\right)(2\phi_{P} - \phi_{L} - \phi_{R})\right]\right\}$$

$$(36)$$

$$+ d_{r}^{u-}\left[\frac{\phi_{L} + \phi_{P}}{2} + \left(\frac{1}{8} + \alpha_{l}\right)(2\phi_{P} - \phi_{L} - \phi_{R})\right]$$

Rearranging this equation and doing the same for the other terms of eqn.

(19), we obtain for the finite-volume equation at P, as in eqn. (20), the coefficients:

$$A_{R} = C_{r}d_{r}^{u+}(-\frac{3}{8} + \alpha_{r}) + C_{r}d_{r}^{u-}(-\frac{6}{8} - 2\alpha_{r}) + C_{l}d_{l}^{u-}(-\frac{1}{8} - \alpha_{l}) + D_{r}$$

$$A_{L} = C_{r}d_{l}^{u+}(\frac{6}{8} + 2\alpha_{l}) + C_{l}d_{l}^{u-}(\frac{3}{8} - \alpha_{l}) + C_{r}d_{r}^{u+}(\frac{1}{8} + \alpha_{r}) + D_{l}$$

$$A_{RR} = C_{r}d_{r}^{u-}(\frac{1}{8} + \alpha_{r})$$

$$A_{LL} = C_{l}d_{l}^{u+}(-\frac{1}{8} - \alpha_{l})$$

$$A_{T} = C_{l}d_{l}^{v+}(-\frac{3}{8} + \alpha_{l}) + C_{l}d_{l}^{v-}(-\frac{6}{8} - 2\alpha_{l}) + C_{b}d_{b}^{v-}(-\frac{1}{8} - \alpha_{b}) + D_{l}$$

$$A_{B} = C_{b}d_{b}^{v+}(\frac{6}{8} + 2\alpha_{b}) + C_{b}d_{b}^{v-}(\frac{3}{8} - \alpha_{b}) + C_{l}d_{l}^{v+}(\frac{1}{8} + \alpha_{l}) + D_{b}$$

$$A_{TT} = C_{l}d_{l}^{v-}(\frac{1}{8} + \alpha_{l})$$

$$A_{BB} = C_{b}d_{b}^{v+}(-\frac{1}{8} - \alpha_{b})$$

$$A_{P} = \sum_{nb} A_{nb}$$

where nb represents (R, L, RR, LL, T, B, TT, BB).

4. Boundary conditions

In order to apply the control-volume method to viscoelastic flow problems based on the above formulation, we need to specify the boundary conditions.

4.1 Velocity

4.1.1 Velocity normal to the boundary

The velocity should be set at its value and no special procedure is needed, except for the outflow condition where the flow is assumed to be fully developed, hence $\partial u/\partial n = 0$, where n is the outward normal direction.

4.1.2 Velocity tangential to the boundary (no slip condition)

The tangential velocity along any solid boundary is prescribed to be equal to zero, that is a non-slip boundary condition is assumed.

4.2 Stresses

The assumption underlying the analytical derivation of boundary values for the stresses is that the constitutive equations hold at the boundary. We shall consider three boundary conditions encountered in this work.

4.2.1 Boundary parallel to the x-axis

In such situations the flow obeys the conditions u = v = 0; $\partial u/\partial x = \partial v/\partial x = 0$; and from the continuity equation $\partial v/\partial y = 0$. Incorporating these conditions in the constitutive equations yields a set of three equations with three unknowns which upon resolution give on the boundary:

$$\tau^{xx} = 2\lambda \mu \left(\frac{\partial u}{\partial y}\right)^2, \qquad \tau^{yy} = 0, \qquad \tau^{xy} = 2\mu \frac{\partial u}{\partial y}$$
(39)

4.2.2 Boundary parallel to the y-axis

In a similar way to the above we find that on this boundary:

$$\tau^{xx} = 0, \qquad \tau^{yy} = 2\lambda\mu \left(\frac{\partial v}{\partial x}\right)^2, \qquad \tau^{xy} = 2\mu\frac{\partial v}{\partial x}$$
 (40)

4.2.3 Re-entrant corners

In this case the velocity derivatives are undefined at the corner. However, a commonly used condition is to set u = v = 0 and solve the resultant set of equations. It is to be noted that due to the staggered-grid configuration only the equation for τ^{xy} uses this boundary condition. The value for τ^{xy} is produced analytically as:

$$\tau^{xy} = \frac{\mu \left(\frac{\partial u}{\partial y} + \frac{\partial v}{\partial x}\right) + 2\lambda \mu \left[\frac{(\partial u/\partial x)(\partial v/\partial x)}{1 - 2\lambda(\partial u/\partial y)} + \frac{(\partial u/\partial y)(\partial v/\partial y)}{1 - 2\lambda(\partial v/\partial x)}\right]}{1 - 2\lambda(\partial u/\partial y)(\partial v/\partial x)\left[\frac{1}{1 - 2\lambda(\partial u/\partial y)} + \frac{1}{1 - 2\lambda(\partial v/\partial x)}\right]}$$
(41)

4.2.4 Entrance conditions

At the entrance the flow is assumed to be fully developed. This assumption yields a simplified set of equations for the stresses, which can be solved analytically with the appropriate values of velocity and velocity gradient at the entrance boundary.

5. The solution algorithm

5.1 The pressure equation

The derivation of a pressure equation to calculate the pressure field is obviously needed. Many algorithms have been developed over the years. The first method for doing this, which was economical in computer time, was proposed by Patankar and Spalding [20] under the acronym SIMPLE (Semi-Implicit Method for the Pressure Linked Equation). Over the years,

a number of modifications to the SIMPLE algorithm have been proposed [11,21,22]. The SIMPLER (SIMPLE Revised) algorithm of Patankar [11] and SIMPLEC (SIMPLE Consistent) algorithm of Van Doormaal and Raithby [22] are examples of such modifications and exhibit better behaviour than SIMPLE and its other variants. However, the approximations needed in the implementation of any of these algorithms are not suited to handling the viscoelastic stress components. Thus an alternative method, which avoids some of the pitfalls encountered in the above methods, the PRIME (PRessure Implicit Momentum Explicit) algorithm [23], is used. Furthermore some modifications were introduced to enhance its efficiency in the calculation of viscoelastic fluids. The reader is referred to Ref. 24 for more details. The PRIME (Modified) algorithm has the following steps:

- 1. Compute the stresses.
- 2. Compute the velocities.
- 3. Compute the pressure and correct the velocities.
- 4. Compute the stresses using the new velocities.
- 5. Compute the pressure and again correct the velocities.
- 6. Return to step 1 until convergence.

5.2 Solution of the discretized equations

The use of direct methods for solving the set of equations described above is not appropriate in the present context because they require too much storage and are usually more time consuming, in particular for the non-linear problems encountered in fluid-flow calculations. Current iterative methods differ with respect to storage requirement and degree of implicitness, such as the point-by-point successive overrelaxation method, the strongly implicit procedure of Stone and its variations, the Incomplete Cholesky Congruent Gradient (ICCG), or the Multigrid Method of Brandt [25]. Although these methods have their own desirable attributes, the degree of simplicity of their implementation in a computer code is approximately inversely proportional to their rate of convergence.

The method adopted in this work is a generalization of the TDMA algorithm for two dimensions, which is easy to program, in combination with an additive-corrective multigrid method [26]. This combination is found to provide the simplicity and low storage needs of the basic TDMA algorithm while preserving the high convergence rate of multigrid methods.

6. Viscoelastic fluid simulation

6.1 The sudden expansion problem

This concerns the flow of an upper-convected Maxwell fluid through a "planar 4:1 sudden expansion" with mean inlet velocity U associated with

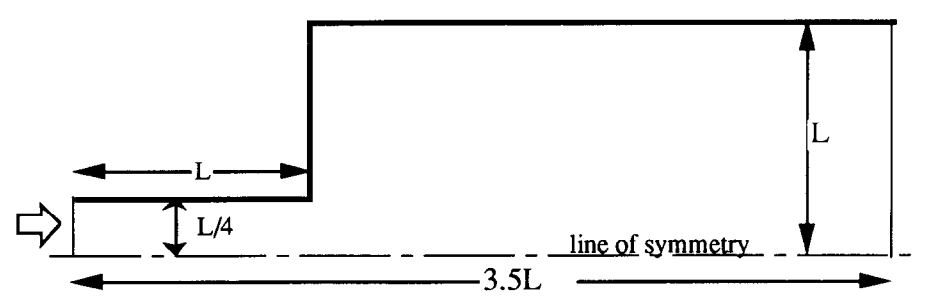


Fig. 4. Geometry of problem 1.

TABLE 1
Conditions for the different cases

Case	U (mean)	ρ	μ	λ	Re	We	Iterations
1	0.01	100	0.125	0	0.1	0	16
2	0.01	100	0.125	1.0	0.1	0.8	+25
3	0.01	100	0.125	3	0.1	2.4	+95

a parabolic inlet velocity profile. The geometry for this problem is shown in Fig. 4. The Reynolds number and Weissenberg number are given by:

$$Re = \frac{\rho UL}{4\mu} \qquad We = \frac{4\lambda U}{L} \tag{42}$$

where the λ and μ values are given in Table 1.

Table 1 shows the different conditions for which solutions were sought. The last column gives the number of iterations required for convergence and increases with the value of We. With L=0.05, a 21×8 mesh with $\Delta x=0.00833$ and $\Delta y=0.00625$ is superposed over the rectangle encompassing the domain of the problem. This will be referred to as Mesh 1.

It is worth noting that the initial guesses used for the pressure, velocity and stress field were, each time, the converged solutions obtained for the previous We. Hence the + sign before the iteration values in Table 1 indicates the extra iterations required for convergence.

Results are shown, in Figs. 5-7, for Re = 0.1 with We = 0, 0.8 and 2.4. In Fig. 6 the velocity-vector field is plotted whilst in Fig. 7 the streamlines are shown for We = 0, 0.8 and 2.4. The effect of the increase in We, which is to suppress the recirculation zone in the upper corner, can be seen in Figs. 6 and 7 for the velocity-vector plots and the velocity streamlines. The

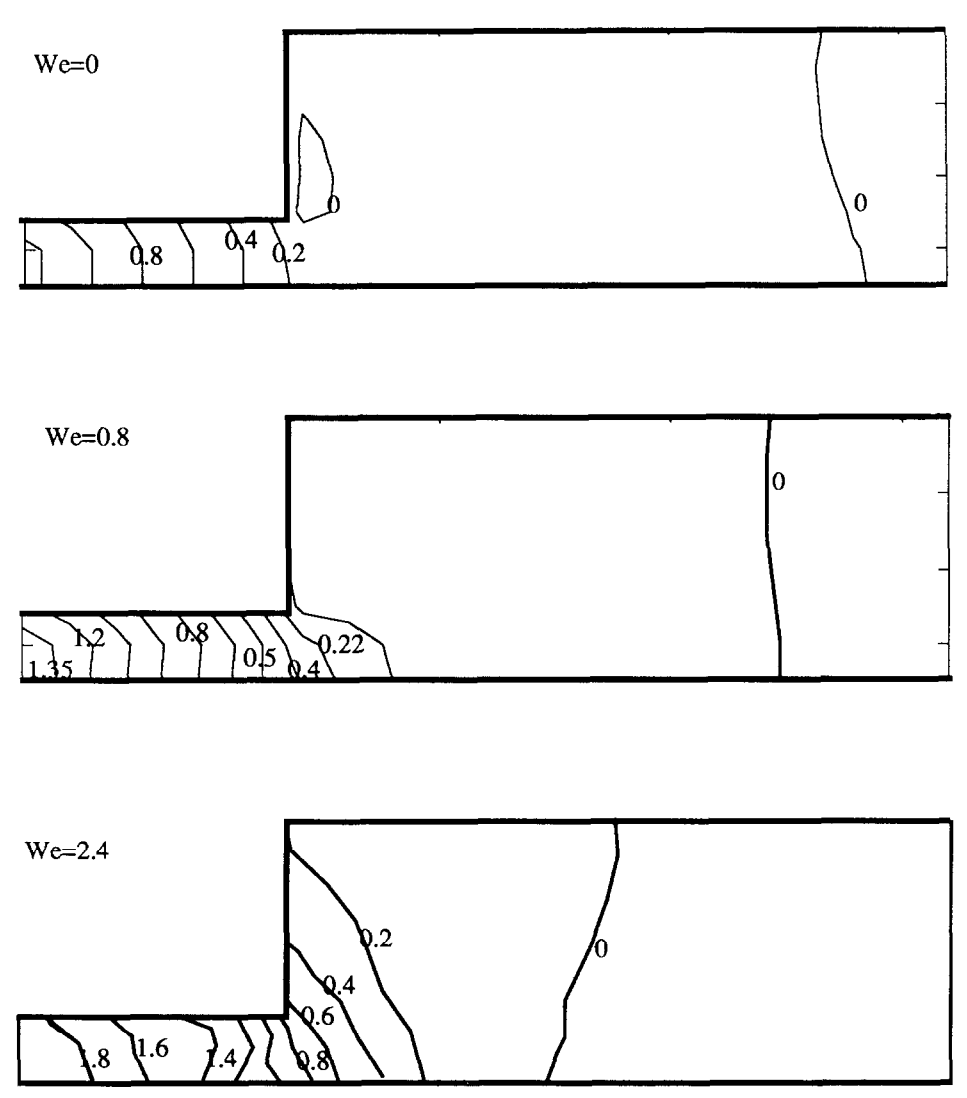
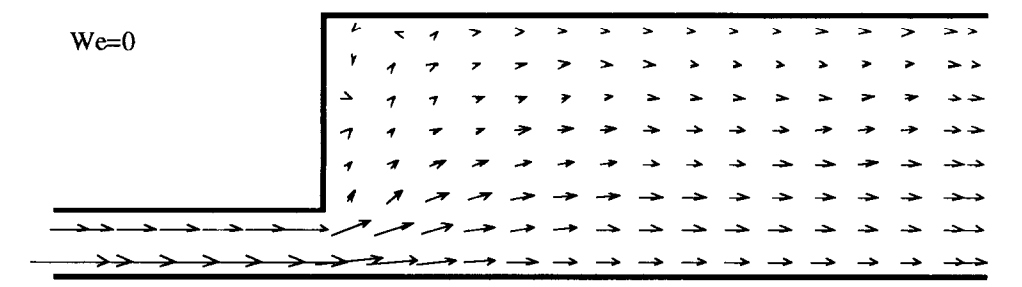
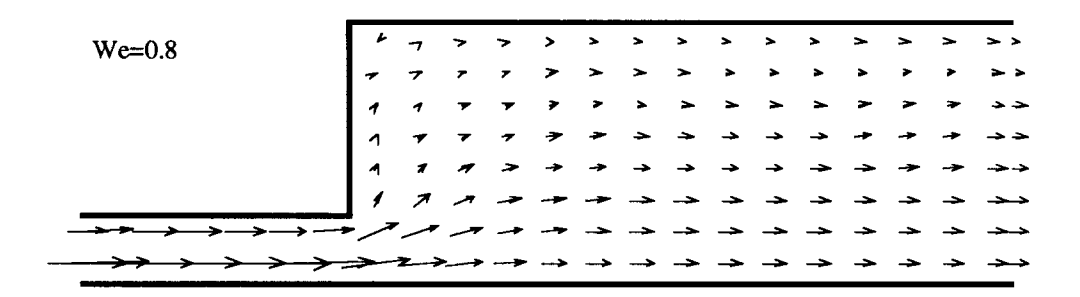


Fig. 5. Pressure contours for Re = 0.1, We = 0, 0.8 and 2.4.

recirculation zone that exists in the Newtonian case for Re = 0.1, disappears for We = 2.4, and the negative pressure region at the expansion zone also disappears. Furthermore the pressure drop across the expansion increases with the We value. Similar effects have been experimentally confirmed recently [27].

The solution of the problem for higher Weissenberg numbers, e.g. We = 3.6, was found to be too time consuming computationally for the PC and was not pursued.





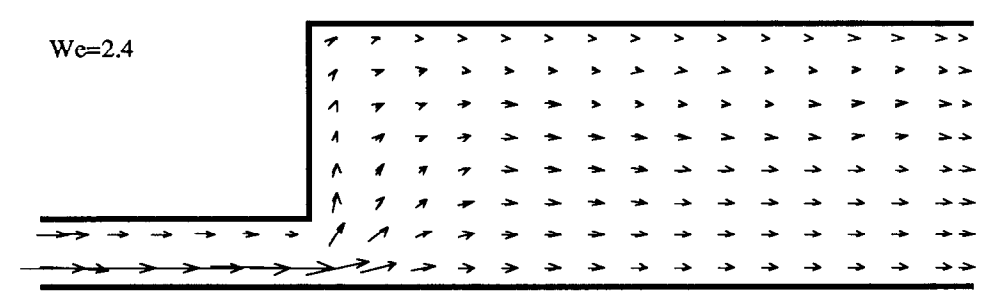
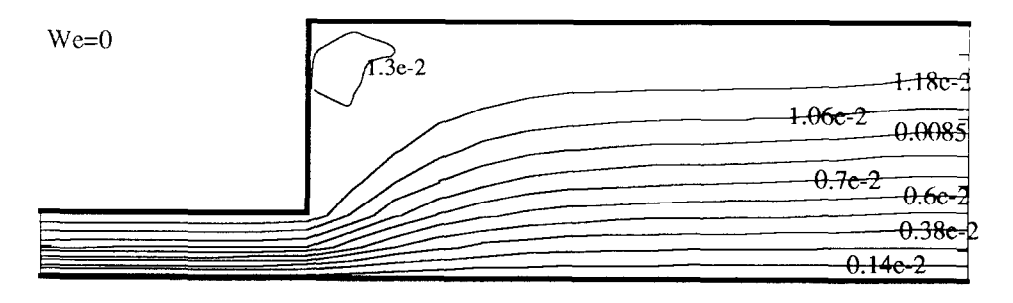
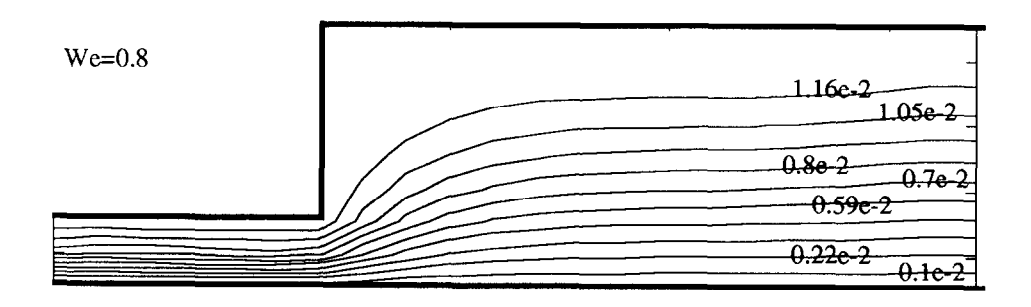


Fig. 6. Velocity-vector plots for Re = 0.1, We = 0, 0.8 and 2.4.

6.2 Mesh refinement

The problem was also solved for a different mesh size based on a 28×12 mesh superposed over the rectangle encompassing the problem domain,





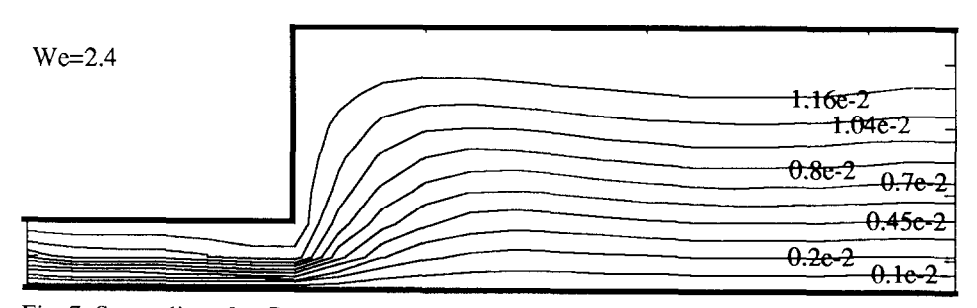


Fig. 7. Streamlines for Re = 0.1, We = 0, 0.8, 2.4.

giving $\Delta x = 0.00625$ and $\Delta y = 0.00417$; this is Mesh 2. The solution for Re = 0.1 and We = 1.2 is shown in Figs. 8-13, for Mesh 1 and Mesh 2.

The values of the parameters used are shown in Table 2.

Figures 8 and 9 show the pressure contours and the velocity-vector plots, respectively, for Mesh 1 and the refined mesh Mesh 2. The suppression of

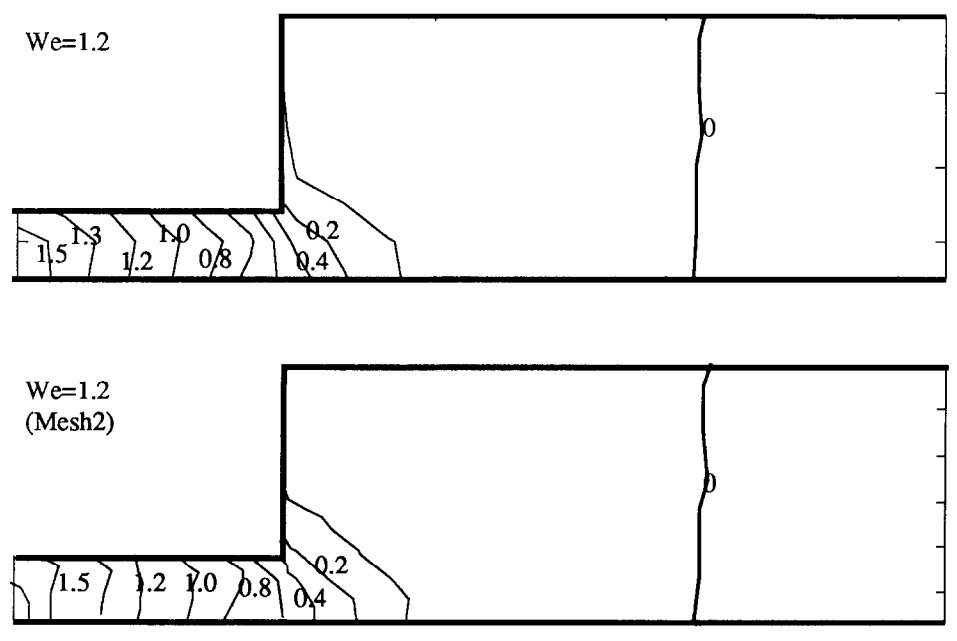


Fig. 8. Pressure contours at Re = 0.1, We = 1.2, for Mesh 1 and Mesh 2.

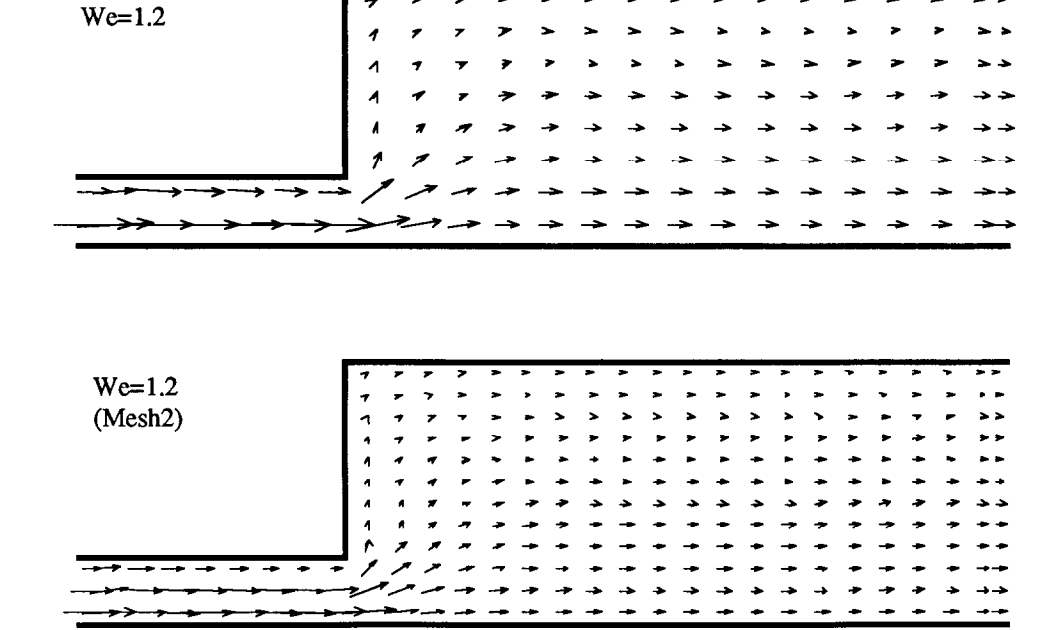


Fig. 9. Velocity-vector plots at Re = 0.1, We = 1.2, for Mesh 1 and Mesh 2.

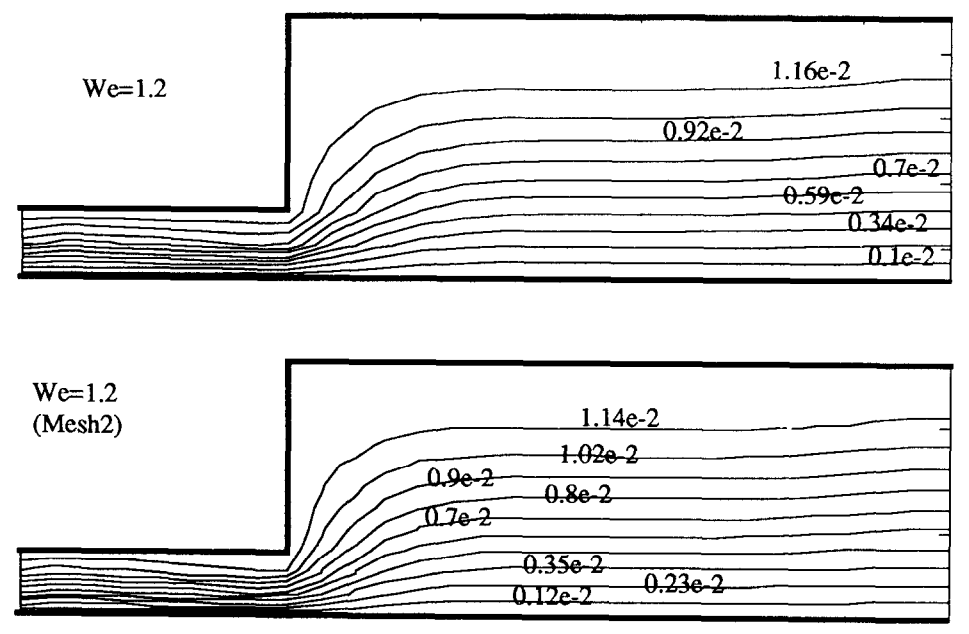


Fig. 10. Streamline contours at Re = 0.1 and We = 1.2, for Mesh 1 and Mesh 2.

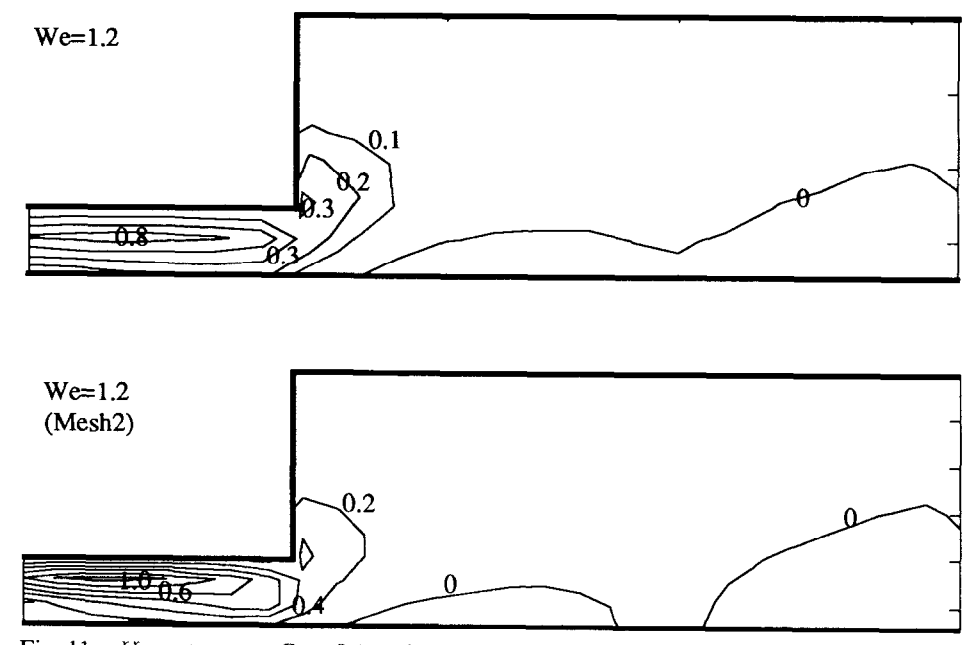


Fig. 11. τ^{xx} contours at Re = 0.1 and We = 1.2, for Mesh 1 and Mesh 2.

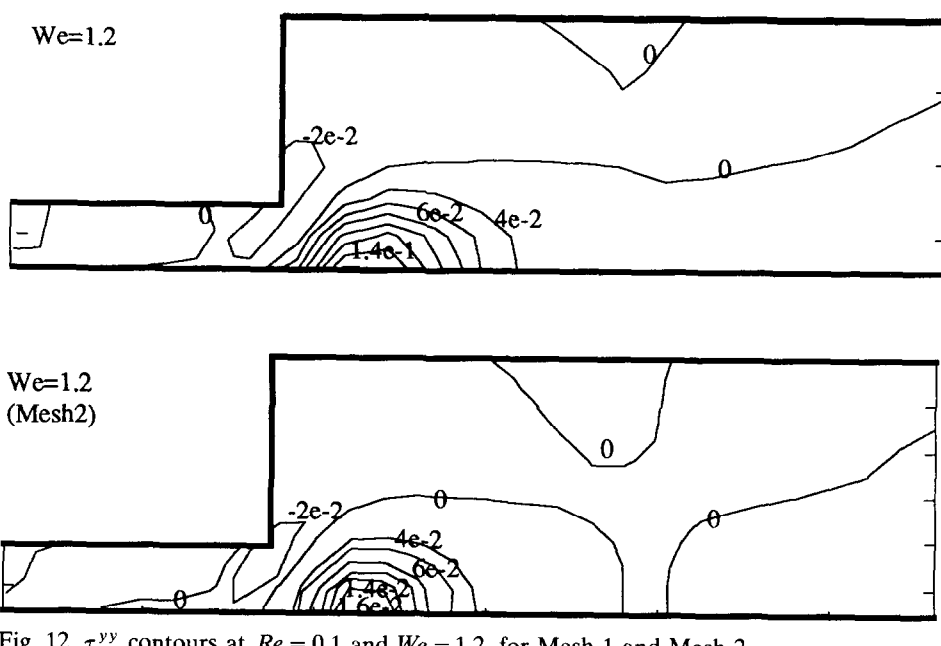
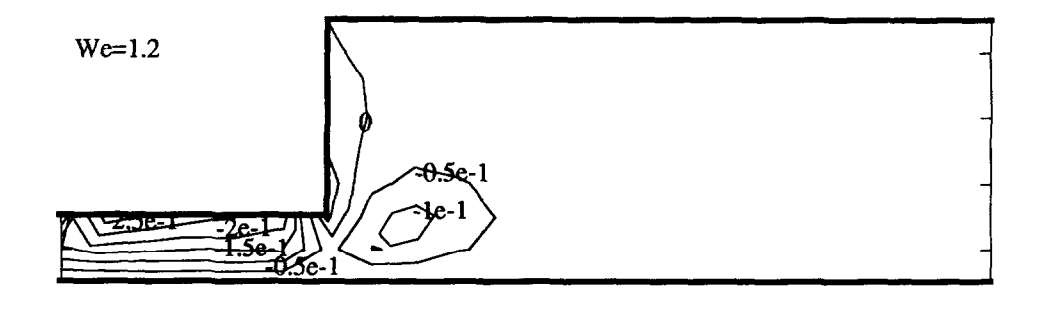


Fig. 12. τ^{yy} contours at Re = 0.1 and We = 1.2, for Mesh 1 and Mesh 2.



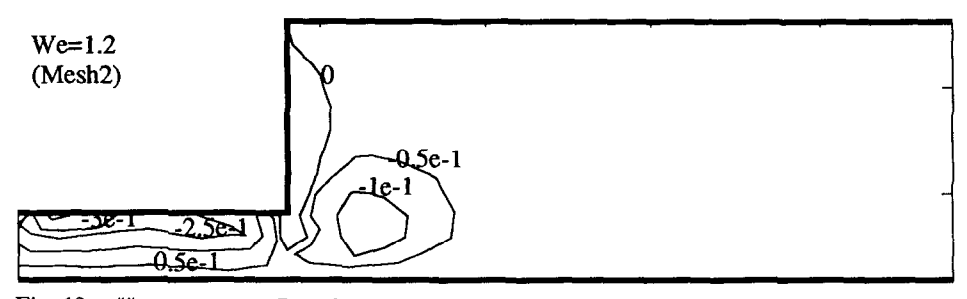


Fig. 13. τ^{xy} contours at Re = 0.1 and We = 1.2, for Mesh 1 and Mesh 2.

U (mean)	ρ	μ	λ	Re	We	Iterations
0.01	100	0.125	1.5	0.1	1.2	+ 55

TABLE 2

Parameter values for mesh refinemen

the recirculation zone is noticed on both meshes, while Fig. 10 shows the streamline contours, also for both meshes. We can see that refinement of the mesh does not filter out the viscoelastic effects obtained on the coarser mesh.

Figures 11, 12 and 13 show the contour plots for the viscoelastic extra-stresses, τ^{xx} , τ^{yy} and τ^{xy} .

7. Conclusion

A decoupled, finite-volume algorithm for solving viscoelastic flows has been described and implemented for two-dimensional problems. This algorithm can immediately be extended to the three-dimensional case. The main features of this algorithm are the use of primitive variables along with a set of specially positioned stress variables, and the use of a third-order upwind scheme for the discretization of the constitutive equations. The advantages are:

- (a) the use of primitive variables will enable the move to three-dimensional models to be performed in a straightforward manner;
- (b) the wealth of experience which evolved in Newtonian computational fluid mechanics can be used in improving the solution procedure in the (still new) computational viscoelastic fluid-dynamics field;
- (c) the implementation of the viscoelastic algorithm in the context of existing codes for simulating the flow of Newtonian fluids should not present major difficulties;
- (d) the Perera and Walters transformation of stresses greatly enhances the stability of the method;
- (e) computer cost is minimal when compared with sub-domain finite-element methods.

It should be remarked that work is also proceeding to apply this control-volume method to problems of sudden contraction, with both planar and axisymmetric geometry to achieve numerical results that agree with experiment; see Darwish et al. [28] for preliminary details.

Acknowledgements

M.S.D. gratefully acknowledges support, in part, by a BTG grant, and J.R.W. support, in part, by the US Army Research, Development and Standardization Group UK under Contract No. DAJA45-89-C-0023.

References

- 1 R.B. Bird, R.C. Armstrong and O. Hassager, Dynamics of Polymeric Liquids, Vol. 1, Fluid Mechanics, John Wiley, 1977.
- 2 M.J. Crochet, A.R. Davies and K. Walters, Numerical Simulation of non-Newtonian Flow, Elsevier, Amsterdam, 1984.
- 3 M.J. Crochet and J.M. Marchal, Recent results on viscoelastic flow calculation, in A.W. Bush, B.A. Lewis and M.D. Warren (Eds.), Flow Modelling in Industrial Processes, Ellis Horwood, 1989.
- 4 M.J. Crochet, Numerical simulation of viscoelastic flow: a review, Rubber Chem. Technol., 62(3) (1989) 426-455.
- 5 A.N. Brooks and T.J.R. Hughes, Streamline upwind/Petrov-Galerkin methods for advection dominated flows. Proc. 3rd Int. Conf. on Finite Element Methods in Fluid Flow, Banff, Canada, 1980.
- 6 T.J.R. Hughes, Recent progress in the development and understanding of SUPG methods, Int. J. Num. Methods Eng., 7 (1987) 1261–1275.
- 7 A.N. Brooks and T.J.R. Hughes, Streamline upwind/Petrov Galerkin formulations for convection dominated flows with particular emphasis on the incompressible Navier– Stokes equations, Comput. Methods Appl. Mech. Eng., 32 (1982) 199–259.
- 8 J.H. Song and J.Y. Yoo, Numerical simulation of viscoelastic flow through sudden contraction using type dependent difference method, J. Non-Newtonian Fluid Mech., 24 (1987) 221-243.
- 9 J.Y. Yoo and Y. Na, A numerical study of the planar contraction flow of a viscoelastic fluid using the SIMPLER algorithm, J. Non-Newtonian Fluid Mech., 39 (1991) 89-106.
- 10 M.G.N. Perera and K. Walters, Long range memory effects in flows involving abrupt changes in geometry, part 1, J. Non-Newtonian Fluid Mech., 2 (1977) 49–81.
- 11 S.V. Patankar, Numerical Heat Transfer and Fluid Flow, Hemisphere Publishing, 1981.
- 12 M.A. Leschziner, Modelling turbulent recirculating flows by finite-volume methods: current status and future directions, Int. J. Heat Fluid Flow, 10 (1989) 186–202.
- 13 D.B. Spalding, A novel finite-difference formulation for differential expressions involving both first and second derivatives, Int. J. Num. Methods Eng., 4 (1972) 551–559.
- 14 M.A. Leschziner, Practical evaluation of three finite difference schemes for the computation of steady-state recirculating flows, Comput. Methods Appl. Mech Eng., 23 (1980) 293–312.
- 15 G.D. Raithby, Skew upwind differencing schemes for problems involving fluid flow, Comput. Methods Appl. Mech. Eng., 19 (1976) 153–164.
- 16 B.P. Leonard, A stable and accurate convective modelling procedure based on quadratic upstream interpolation, Comput. Methods Appl. Mech. Eng, 19 (1979) 59–98.
- 17 P.H. Gaskell and A.K.C. Lau, Curvature-compensated convective transport: SMART, a new boundedness-preserving transport algorithm, Int. J. Num. Methods Fluids, 8 (1988) 617–641.
- 18 B.P. Leonard, M.A. Leschziner and J. McGuirk, Third order finite-difference method

- for steady two-dimensional convection, in C. Taylor, K. Morgan and C.A. Brebbia (Eds.), Numerical Methods in Laminar and Turbulent Flows, Pentech Press, 1978, pp. 807–819.
- 19 B.P. Leonard, The Euler-QUICK code, in C. Taylor, A.A. Johnson and W.R. Smith (Eds.), Numerical Methods in Laminar and Turbulent Flow, Wiley, Chichester, 1983, pp. 489-499.
- 20 S.V. Patankar and D.B. Spalding, A calculation procedure for heat, mass and momentum transfer in three-dimensional parabolic flows, Int. J. Heat Mass Transfer, 15 (1972) 1787–1806.
- 21 G.D. Raithby and G.E. Schneider, Numerical solution of problems in incompressible fluid flow: treatment of the velocity-pressure coupling, Num. Heat Transfer, 2(2) (1979) 417-440.
- 22 J.P. Van Doormaal and G.D. Raithby, Enhancement of the SIMPLE method for predicting incompressible fluid flows, Num. Heat Transfer, 7 (1984) 147-163.
- 23 C.R. Maliska and G.D. Raithby, Calculating 3D fluid flows using orthogonal grids, Proc. Third Int. Conf. Num. Methods in Laminar and Turbulent Flows, Seattle, WA, (1986) pp. 656-666.
- 24 M.S. Darwish, On new routes for the management of fibre orientation in extrusion processes and the simulation of viscoelastic fluids, Ph.D. Thesis, Brunel University, Uxbridge, UK, 1991.
- 25 A. Brandt, Multi-level adaptive solutions to boundary-value problems, Math. Comput., 31 (1977) 333–390.
- 26 B.R. Hutchinson and G.D. Raithby, A multigrid based on the additive correction strategy, Num. Heat Transfer, 9 (1986) 511-537.
- 27 A.R. Davies, personal communication, Aberystwyth, The University College of Wales.
- 28 M.S. Darwish, J.R. Whiteman and M.J. Bevis, Numerical modelling of viscoelastic liquids using a finite volume method, Institute of Computational Mathematics, Brunel University, Technical Report: BICOM 91/5, August 1991.
- 29 B.P. Leonard, SHARP simulation of discontinuities in highly convective steady flow, NASA Technical Memorandum 100240, ICOMP-87-9, 1987.

Appendix: The normalized variable diagram

The QUICK interpolation profile at some control-volume face involves the two adjacent node values ($\phi_{Downstream}$) and (ϕ_{Middle}) together with that at the next upstream mode ($\phi_{Upstream}$) as seen in Fig. A1. Note that the labelling of the nodes as Downstream, Upstream and Middle depends on the velocity direction, as was described in Section 3. Leonard [19] defined a normalized variable through which the information provided by the three nodes can be related to one parameter; the form of this normalized variable is

$$\tilde{\phi} = \frac{\phi - \phi_{\text{Upstream}}}{\phi_{\text{Downstream}} - \phi_{\text{Upstream}}} \tag{A1}$$

Note that using normalized variables we have $\tilde{\phi}_{\text{Downstream}} = 1$ and $\tilde{\phi}_{\text{Upstream}} = 0$ (see Fig. A1).

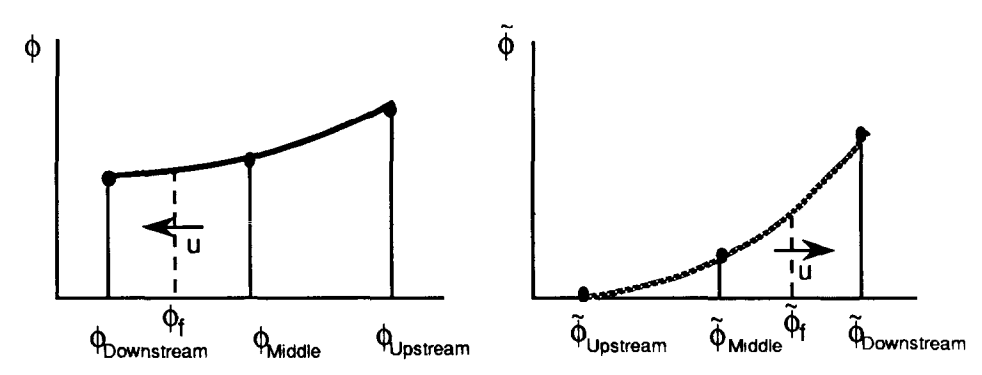


Fig. A1. Normalized variables (right).

The QUICK scheme with the normalized variables is thus written at some control volume face, f, as

$$\tilde{\phi}_f = \frac{3}{8} + \frac{3}{4} \tilde{\phi}_{\text{Middle}} \tag{A2}$$

Other schemes can be written in a normalized form. For the upwind scheme we have:

$$\tilde{\phi}_f = \tilde{\phi}_{\text{Middle}} \tag{A3}$$

whilst the central difference scheme can be written as:

$$\tilde{\phi}_f = \frac{1}{2} + \frac{1}{2} \tilde{\phi}_{\text{Middle}} \tag{A4}$$

and the second-order upwind scheme:

$$\tilde{\phi}_f = \frac{3}{2} \tilde{\phi}_{\text{Middle}} \tag{A5}$$

Plots of these relations for $\tilde{\phi}_f$ against $\tilde{\phi}_{\text{Middle}}$ are given in Fig. A2.

Leonard has shown [19] that unphysical behaviour is related to schemes that pass through the second quadrant of the normalized variable diagram, or pass above point P in the first quadrant, while schemes that pass in the fourth quadrant are artificially diffusive. On the other hand, for a scheme to have a second-order accuracy it is sufficient that is passes through the point Q, and that passing through Q with a slope of 3/4 is necessary and sufficient for third-order accuracy.

With this in mind, it is easy to see how the QUICK scheme can be modified to eliminate some of its unwanted behaviour. Figure A3 shows the SMART scheme of Gaskel and Lau which involves modifying the QUICK scheme in two places in the first quadrant so as to make it pass through points O and P. The changes beyond point P and in the third quadrant were incorporated from the SHARP scheme of Leonard [29]. The

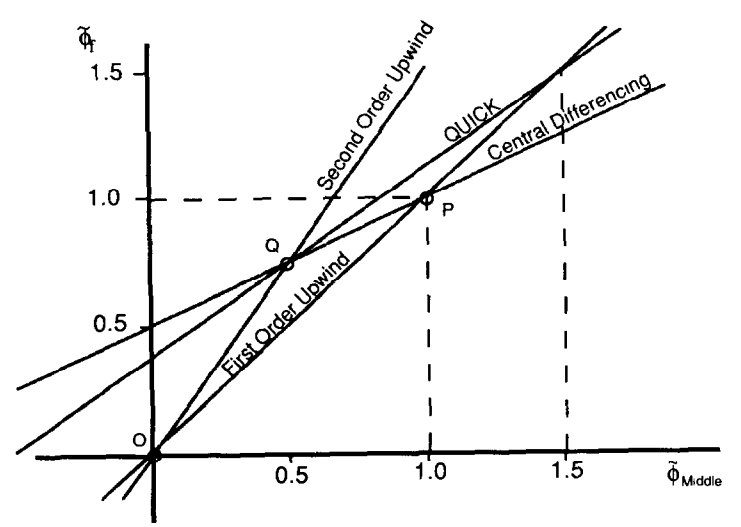


Fig. A2. The normalized variable diagram for different interpolation schemes.

effects of the above-mentioned modifications are carried through the α parameter into the SMART scheme which can be written as a function of the normalized variable as

$$\tilde{\phi}_f = \frac{3}{8} + \frac{3}{4} \tilde{\phi}_{\text{Middle}} - \alpha_f \left(1 - 2 \tilde{\phi}_{\text{Middle}} \right) \tag{A6}$$

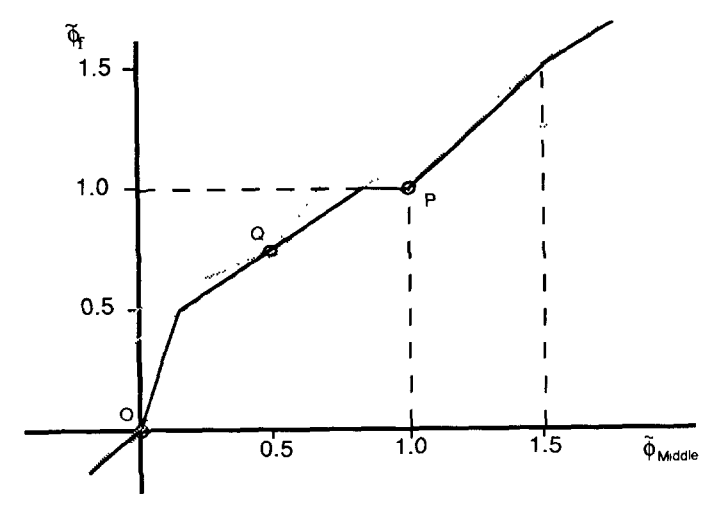


Fig. A3. The normalized variable diagram for the SMART scheme.

The actual relation between $\tilde{\phi}_f$ and $\tilde{\phi}_{\text{Middle}}$ for the SMART scheme is defined as follows:

$$\begin{split} \tilde{\phi}_f = f \Big(\tilde{\phi}_{\text{Middle}} \Big) \begin{cases} &= \tilde{\phi}_{\text{Middle}} & \text{if } -1 < \tilde{\phi}_{\text{Middle}} \leq 0 \\ &= 3 \tilde{\phi}_{\text{Middle}} & \text{if } 0 < \tilde{\phi}_{\text{Middle}} \leq \frac{1}{6} \\ &= 1 & \text{if } \frac{5}{6} < \tilde{\phi}_{\text{Middle}} \leq 1 \\ &= \tilde{\phi}_{\text{Middle}} & \text{if } 1 < \tilde{\phi}_{\text{Middle}} \leq \frac{3}{2} \\ &= \frac{3}{8} \Big(2 \tilde{\phi}_{\text{Middle}} + 1 \Big) & \text{for all other cases} \end{cases} \end{split} \tag{A7}$$

The values of α needed to satisfy the above relation can now be obtained. After manipulation of eqn. (A6) we get:

$$\alpha_f = g(\tilde{\phi}_f, \, \tilde{\phi}_{\text{Middle}}) = \left(\frac{\tilde{\phi}_f - \frac{3}{8}(2\tilde{\phi}_{\text{Middle}} + 1)}{2\tilde{\phi}_{\text{Middle}} - 1}\right) \tag{A8}$$

and using the relations of eqn. (A7) we get the following relation:

$$\alpha_{f} = g'(\tilde{\phi}_{\text{Middle}})$$
 if $-1 < \tilde{\phi}_{f} \le 0$

$$= \frac{3}{4} \frac{\left(3\tilde{\phi}_{\text{Middle}} - 0.5\right)}{\left(2\tilde{\phi}_{\text{Middle}} - 1\right)}$$
 if $0 < \tilde{\phi}_{\text{Middle}} \le \frac{1}{6}$

$$= \frac{1}{8} \frac{5 - 6\tilde{\phi}_{\text{Middle}} - 1}{2\tilde{\phi}_{\text{Middle}} - 1}$$
 if $0 < \tilde{\phi}_{\text{Middle}} \le 1$

$$= \frac{1}{8} \frac{2\tilde{\phi}_{\text{Middle}} - 3}{2\tilde{\phi}_{\text{Middle}} - 1}$$
 if $1 < \tilde{\phi}_{\text{Middle}} \le \frac{3}{2}$

$$= 0$$
 for all other cases

During each iteration or time step the coefficients of the control volume equations are calculated using the QUICK scheme and then the normalized variable for each face is calculated, using eqn. (A1). The value of α at this face is obtained and the coefficient of the control volume equations corrected. By changing the relation of eqn. (A9) many different schemes can be produced by changing only one subroutine in the whole program; hence another advantage of this technique.